Cellular Physiology and Biochemistry

Cell Physiol Biochem 2018;48:1843-1853
DOI: 10.1159/000492506
Published online: August 8, 2018
Accepted: July 30, 2018

Original Paper

Aldehyde Dehydrogenase-2 Attenuates Myocardial Remodeling and Contractile Dysfunction Induced by a High-Fat Diet

Chuanbao Li[a,b,c] Xiaoxing Li[c,d] Ying Chang[a,b,c] Lang Zhao[c] Baoshan Liu[a,b,c] Shujian Wei[a,b,c] Feng Xu[a,b,c] Yun Zhang[c] Yuguo Chen[a,b,c]

[a]Department of Emergency Medicine and Chest Pain Center, Qilu Hospital, Shandong University, Jinan, [b]Key Laboratory of Emergency and Critical Care Medicine of Shandong Province, Qilu Hospital, Shandong University, Jinan, [c]The Key Laboratory of Cardiovascular Remodeling and Function Research, Chinese Ministry of Education and Chinese Ministry of Public Health, Qilu Hospital, Shandong University, Jinan, [d]Department of Geriatrics, Qilu Hospital, Shandong University, Jinan, China

Key Words
Metabolic syndrome • Myocardial remodeling • Apoptosis • ALDH2 • Mice

Abstract
Background/Aims: Consumption of a high-fat (HF) diet exacerbates metabolic cardiomyopathy through lipotoxic mechanisms. In this study, we explored the role of aldehyde dehydrogenase-2 (ALDH2) in myocardial damage induced by a HF diet. ***Methods:*** Wild-type C57 BL/6J mice were fed a HF diet or control diet for 16 weeks. ALDH2 overexpression was achieved by injecting a lentiviral ALDH2 expression vector into the left ventricle. ***Results:*** Consumption of a HF diet induced metabolic syndrome and myocardial remodeling, and these deleterious effects were attenuated by ALDH2 overexpression. In addition, ALDH2 overexpression attenuated the cellular apoptosis and insulin resistance associated with a HF diet. Mechanistically, ALDH2 overexpression inhibited the expression of c-Jun N-terminal kinase (JNK)-1, activated protein 1 (AP-1), insulin receptor substrate 1 (IRS-1), 4- hydroxynonenal, caspase 3, transforming growth factor β1, and collagen I and III, and enhanced Akt phosphorylation. ***Conclusion:*** ALDH2 may effectively attenuate myocardial remodeling and contractile defects induced by a HF diet through the regulation of the JNK/AP-1 and IRS-1/Akt signaling pathways. Our study demonstrates that ALDH2 plays an essential role in protecting cardiac function from lipotoxic cardiomyopathy.

Yuguo Chen MD, PhD
and Xiaoxing Li MD, PhD.

Qilu Hospital, Shandong University
107 Wenhua Xi Road, Jinan, Shandong 250012 (China)
E-Mail yuguochen@hotmail.com, lxx2010@126.com

Introduction

Chronic consumption of a high-fat (HF) diet leads to metabolic syndrome (MS), which is characterized by a number of metabolic disorders, including obesity, impaired glucose tolerance, and high triglyceride levels [1]. Obesity induced by a HF diet is associated with the increased generation of reactive oxygen species (ROS), which induce oxidative stress in the body [2]. The oxidative stress induced by obesity causes cardiovascular complications, including lipotoxic cardiomyopathy, which can manifest as myocardial remodeling and cardiac dysfunction [3]. Previous studies have shown that glucose/lipid metabolism disorder and hypertension contribute to changes in left ventricular structure and function [4-6].

Mitochondrial aldehyde dehydrogenase type 2 (ALDH2) is a key enzyme involved in cardiac protection [7]. ALDH2 activation correlates strongly with cardioprotective effects in a number of model systems [8-10]. ALDH2 is activated by several pathways, including the c-Jun N-terminal kinase (JNK)/activated protein-1 (AP-1) pathway, which plays an important role in cardiac remodeling and cellular apoptosis [11, 12]. JNK regulates the activity of numerous mitochondrial and nuclear proteins by phosphorylation [13]. In particular, the JNK/AP-1 signaling pathway may facilitate the insulin resistance and myocardial hypertrophy induced by oxidative stress [14, 15]. Furthermore, insulin receptor substrate 1 (IRS-1) and serine-threonine protein kinase Akt regulate the insulin resistance and cell apoptosis associated with oxidative stress [16, 17]. ALDH2 protects against cardiac abnormalities in HF diet induced obesity through a mechanism related to autophagy regulation and SUV39H-Sirt1-dependent PGC-1α deacetylation [18]. However, it remains unclear whether ALDH2 regulates the JNK/AP-1 or IRS-1/Akt signaling pathways during myocardial remodeling induced by MS.

In this study, we investigated the protective role of ALDH2 in lipotoxic cardiomyopathy induced by MS, and we explored the underlying signaling mechanism. We produced a mouse model of MS; we overexpressed ALDH2 in this model to determine whether ALDH2 inhibits oxidative stress and insulin resistance and protects against cardiac dysfunction and myocardial tissue damage induced by a HF diet. In addition, we explored the mechanisms of cardioprotection associated with ALDH2 overexpression, with particular focus on the JNK/AP-1 and IRS-1/Akt signaling pathways.

Materials and Methods

Experimental animals

All animal care and experimental protocols complied with the guidelines for the care and use of laboratory animals of Shandong University. The mice were housed in a temperature-controlled environment with a 12-h light, 12-h dark cycle, and had access to water and food *ad libitum*. The mice in the control group (NC group) were fed standard chow and tap water, while the mice in the experimental group were fed a HF diet. After 16 weeks, the mice were evaluated for MS using criteria analogous to those of Adult Treatment Panel III. A diagnosis of MS was indicated by the presence of ≥3 of the following pathological features: high fasting glucose, hypertriglyceridemia, low high-density lipoprotein–cholesterol (HDL-C), excessive waist circumference, or hypertension. A total of 43 mice were found to exhibit symptoms of MS and were divided into three groups: the MS group (n=15), which continued to be fed a HF diet and received the injection of normal saline into the left ventricle; the green fluorescent protein (GFP) vector control group (n=14), which continued to be fed a HF-diet and received an injection of the GFP lentiviral control vector into the left ventricle; and the ALDH2 group (n=14), which continued to be fed a HF-diet and received an injection of the ALDH2 lentiviral vector into the left ventricle. The mice were anesthetized with 1% isoflurane prior to injection. To inject into the left ventricle, the heart was exteriorized by anterior thoracotomy. A 25-μL volume of lentivirus solution or normal saline was injected quickly into three different locations in the left ventricle using a 1-ml syringe. After the injection, the pneumothorax was evacuated and the chest was closed.

Bodyweight measurement and serologic examination

On a monthly basis, venous blood was collected after overnight fasting. Fasting concentrations of serum cholesterol, triglycerides (TG), low-density lipoprotein–cholesterol (LDL-C), HDL-C, fasting blood glucose (FBG), and fasting insulin (FINS) were evaluated at the Department Clinical Laboratory (Qilu Hospital affiliated with Shandong University, Jinan, China). The insulin resistance index (IRI) was calculated according to the following formula: IRI= (FBG × FINS)/22.5, as described previously [19].

Echocardiographic assessment

To examine cardiac structure and function, mice were anesthetized by 1% isoflurane and evaluated using two-dimensional guided M-mode echocardiography on a Vevo 770 instrument equipped with a 30 MHz transducer (RMV 707B; Visual Sonics, Toronto, Canada). Left ventricular end-diastolic diameter (LVEDD), left ventricular end-systolic diameter (LVESD), left ventricular end-diastolic volume (LVEDV), left ventricular end-systolic volume (LVESV), interventricular septal thickness (IVSd) and left ventricular posterior wall thickness at end diastole (LVPWd) were recorded from the M-mode images. Ejection fraction (EF) and fractional shortening (FS) were calculated as follows: EF = (LVEDV−LVESV)/LVEDV×l00%; FS = (LVEDD−LVESD)/LVEDD×l00%, as described previously [20]. All echocardiograms were performed by one experienced individual using a hand-held probe. Parameters were measured over five consecutive cycles.

Histological examination

Following anesthesia and euthanasia, a portion of the left ventricle was excised, rinsed with phosphate-buffered saline (PBS), and fixed immediately in 10% neutral-buffered formalin. The specimens were embedded in paraffin, cut into 5-μm sections, and stained with hematoxylin and eosin (HE) and Masson's trichrome (Sigma-Aldrich, St. Louis, MO). The percentage of Masson blue staining was measured in 10 randomly selected fields on each section of three non-consecutive serial sections from each mouse. The remaining heart tissue was frozen at -80°C for western blotting and detection of ALDH2 enzymatic activity.

Transmission electron microscopy

A portion of the myocardium of approximately 2.5 mm^3 was fixed with 2.0% glutaraldehyde for examination by electron microscopy. The sections were examined on an H-7000FA transmission electron microscope (Hitachi Co. Ltd., Tokyo, Japan).

Measurement of mitochondrial ALDH2 activity

Mitochondrial ALDH2 activity was measured at room temperature in a buffer containing 33 mM sodium pyrophosphate, 0.8 mM NAD^+, 15 mM propionaldehyde, and 50 μg protein. The substrate of ALDH2 was oxidized to acetic acid, while NAD^+ was reduced to NADH. NADH production was determined by measuring absorbance at 340 nm. ALDH2 activity was expressed as nmol NADH produced per min per mg protein.

Terminal deoxynucleotidyl transferase-mediated dUTP nick end labeling assay

Sections of ventricular tissue (5 μm thick) were paraffin-embedded and incubated in a proteinase K solution for 30 min. The sections were then stained with a terminal deoxynucleotidyl transferase mediated dUTP nick end labeling (TUNEL) kit (Roche, Basel, Switzerland) following the manufacturer's protocols. Nuclei were identified by DAPI staining. TUNEL-positive cells were counted using a fluorescence microscope (Olympus, Tokyo, Japan) at 400× magnification, and the percentage of apoptotic cells was calculated.

Measurement of mitochondrial membrane potential

Changes in mitochondrial membrane potential (ΔΨm) were determined using the JC-1 fluorescent probe (Life Technologies, Carlsbad, CA). Purified mitochondria were stained with JC-1 at 37°C for 20 min and analyzed by flow cytometry (FACSCalibur; BD, Franklin Lakes, NJ) or by confocal microscopy. Fluorescence emission was measured at 530 nm for the monomer form of JC-1 (green), and at 590 nm for JC-1 aggregates (red). A reduction in ΔΨm is indicated by a decrease in fluorescence at 590 nm.

Measurement of ROS

Dichlorodihydrofluorescein diacetate (DCFH-DA) fluorescence (Life Technologies) was used to measure intracellular ROS. Cardiomyocytes were incubated with 5 mM DCFH-DA for 20 min at 37°C in Hank's balanced salt solution, rinsed with PBS, recovered in complete Dulbecco's modified Eagle's medium, and analyzed immediately with a laser-scanning confocal microscope (Model LSM710; Zeiss, Jena, Germany). Fluorescence intensity was measured using Image-Pro Plus software (Media Cybernetics, Atlanta, GA).

Immunohistochemical staining

After the sections were dewaxed and rehydrated, antigen retrieval was performed for 15 min in 1% citric acid buffer (pH 6.0) at 92–98°C. The slides were cooled at room temperature for 30 min, rinsed with PBS, and incubated for 20 min with 5% bovine serum albumen to block nonspecific binding. The slides were incubated with an anti-4-hydroxynonenal (4-HNE) antibody (1:200; rabbit polyclonal anti-mouse; Sigma-Aldrich) overnight at 4°C, and then incubated with biotinylated anti-rabbit IgG secondary antibody. A DAB substrate kit (Vector Laboratories, Burlingame, CA) was used to detect the immunohistochemical reaction.

Western blot analysis

Proteins were separated by sodium dodecyl sulfate-polyacrylamide gel electrophoresis and transferred to nitrocellulose membranes. The membranes were blocked with 5% nonfat milk and incubated with specific primary antibodies overnight at 4°C. Antibodies against p-JNK, IRS-1, p-IRS-1, Akt, and p-Akt were purchased from Cell Signaling Technology (Beverly, MA), and antibodies against ALDH2 and caspase 3 were obtained from Santa Cruz Biotechnology (Santa Cruz, CA). An anti-AP-1 antibody was purchased from Abcam (Cambridge, MA). The membranes were incubated with horseradish peroxidase-coupled secondary antibodies. The membranes were developed using ECL Prime reagents (GE Healthcare, Piscataway, NJ) and chemiluminescence was detected using a LAS-4000 luminescent image analyzer (Fujifilm, Stamford, CT, USA). Densitometry analysis was performed using ImageJ software (National Institutes of Health, Bethesda, MA).

Real-time PCR

The TRIzol reagent (Invitrogen) was used to extract total RNA. Total RNA concentration was determined using a NanoDrop ND-1000 spectrophotometer (NanoDrop Technologies, Wilmington, DE). First strand cDNA synthesis was performed using random primers and TaqMan reverse transcription reagents (Applied Biosystems, Foster City, CA). Real-time PCR was performed using predesigned TaqMan probe-primer sets and the Gene Expression Master Mix (Applied Biosystems) in a Prism 7500 system (Applied Biosystems), with the exception of DLL4, which was measured by the SYBR Green method using SsoFast EvaGreen Supermix (Bio-Rad Laboratories, Hercules, CA). The sequence of specific primers were as follows: collagen I: sense 5′-GTTCCTCCCAGCTCTCCATCAAGA-3′ and antisense 5′-GCTCTGGTCACAGGGTCTCATCTC-3′; collagen III: sense 5′-GGCTTCCTGCTCTTCCATCTCTTA-3′ and antisense 5′-CCTTCTCTAGGCGGCAAGTGACCT-3′; and transforming growth factor (TGF)-β1: sense 5′-TTGCTTCAGCTCCACAGAGA-3′ and antisense 5′-TGGTTGTAGAGGGCAAGGAC-3′. mRNA levels were normalized to β-actin. Relative mRNA expression was assessed using the $2^{-\Delta\Delta Ct}$ method.

Statistical analysis

Data are presented as the mean ± standard error of the mean (SEM). Comparisons were performed using one-way analysis of variance followed by a Tukey–Kramer post hoc test. $P < 0.05$ was considered statistically significant.

Results

ALDH2 improves the metabolic index of MS mice

Mice fed a HF diet had higher CHO, triglycerides, LDL-C, FBG, and FINS levels, and an elevated homeostatic model assessment of insulin resistance index compared with mice fed a normal diet (Table 1). The mice in the HF diet group gained more weight than those in the normal diet group (Table 1). After the injection of lentiviral vector, the mice in the ALDH2-

overexpression group exhibited the greatest decreases in these factors from baseline compared with the MS group. Furthermore, ALDH2 overexpression improved the metabolic index (Table 1).

ALDH2 improves the echocardiographic index in MS mice

The mice fed a HF diet exhibited significantly elevated LVEDD, LVESD, IVSd, and LVPWd and reduced EF and FS, and these effects were mitigated by ALDH2 overexpression. Additionally, compared with the MS mice, ALDH2 overexpression significantly slowed the progression of cardiac dysfunction (Table 2).

As expected, injection of the ALDH2-overexpression lentivirus significantly increased cardiac ALDH2 expression and ALDH2 enzymatic activity (Fig. 1A,B). ALDH2 activity in cardiac mitochondria from mice with MS was markedly diminished compared with mice fed a normal diet (NC group) (Fig. 1B). Interestingly, we observed a positive correlation between ALDH2 activity and EF (Fig. 1C).

Table 1. General characteristics of the four groups before and after injection of the lentiviral vector. Data are expressed as the mean ± SEM. BW: body weight; FBG: fasting blood glucose; FINS : fasting insulin; TG : triglyceride; TC: total cholesterol; LDL-C: low density lipoprotein-cholesterol; IRI: insulin resistance index. **P < 0.01 and *P < 0.05, vs. NC group;$^{\#\#}$P < 0.01 and $^{\#}$P < 0.05 vs. MS group; $^{\$\$}$ P < 0.01 and $^{\$}$ P < 0.05 vs. GFP group

	Before injection				After injection			
	NC (n=15)	MS (n=14)	ALDH2(n=14)	GFP (n=14)	NC (n=15)	MS (n=14)	ALDH2 (n=14)	GFP (n=14)
BW (g)	25.03±1.65	31.69±2.25**	30.72±1.82**	30.69±2.07**	25.47±1.96	33.88±2.11**	29.73±1.99**$^{\#\#\$}$	31.46±1.81**
TC (mmol/L)	3.28±0.22	4.54±0.24**	4.51±0.19**	4.46±0.21**	3.21±0.23	4.88±0.29**	4.08±0.21**$^{\#\#\$\$}$	4.76±0.22**
TG (mmol/L)	0.85±0.26	1.17±0.22**	1.20±0.35**	1.21±0.23**	0.90±0.26	1.24±0.33**	1.01±0.16**$^{\#\$}$	1.23±0.21**
LDL-C (mmol/L)	0.36±0.06	0.64±0.05**	0.66±0.09**	0.64±0.08**	0.39±0.06	0.74±0.04**	0.58±0.06**$^{\#\#\$\$}$	0.72±0.05**
FBG (mmol/L)	5.86±1.86	9.45±1.23**	8.97±1.24**	9.35±0.82**	6.65±1.86	11.30±1.03**	8.80±0.93**$^{\#\#\$\$}$	10.21±0.95**
FINS (μIU/l)	18.47±4.18	23.49±3.81**	24.46±5.28**	23.03±5.02**	21.90±3.18	31.68±5.28**	24.39±6.30$^{\#\#\$\$}$	30.70±7.10**
IRI	4.81±1.99	9.87±2.20**	9.74±2.51**	9.56±2.19**	6.41±1.73	15.89±2.98**	9.52±2.58**$^{\#\#\$\$}$	13.88±3.23**

Table 2. Echocardiographic measurements in the four groups of mice at the end of the experiment. Data are expressed as the mean ± SEM. HR: heart rate; bmp: beats per minute; IVSd: interventricular septal thickness at end diastole; LVPWd:left ventricular posterior wall thickness at end diastole;LVEDD: left ventricular end-diastolic dimension; LVESD: left ventricular end-systolic dimension; EF: ejection fraction; FS: fractional shortening. **P < 0.01 and *P < 0.05 vs. NC group; $^{\#\#}$P < 0.01 and $^{\#}$P < 0.05 vs. MS group; $^{\$\$}$ P < 0.01 and $^{\$}$ P < 0.05 vs. GFP group

	NC (n=15)	MS (n=14)	ALDH2 (n=14)	GFP (n=14)
HR(bpm)	457.31±28.56	489.17±30.21	465.13±29.32	491.25±31.16
IVSd(mm)	0.61±0.01	0.89±0.03*	0.68±0.02$^{\#\$}$	0.91±0.03*
LVPWd(mm)	0.58±0.01	0.85±0.03*	0.67±0.02$^{\#\$}$	0.87±0.03*
LVEDD (mm)	3.43±0.34	3.94±0.31**	3.67±0.38**$^{\#\$}$	3.99±0.29**
LVESD (mm)	2.07±0.21	2.59±0.14**	2.50±0.30**	2.62±0.22**
EF (%)	72.16±5.68	61.37±8.20**	66.74±7.35**$^{\#\$}$	59.57±4.49**
FS (%)	42.93±3.64	32.02±3.08**	36.84±4.15**$^{\#\#\$}$	33.72±3.28**

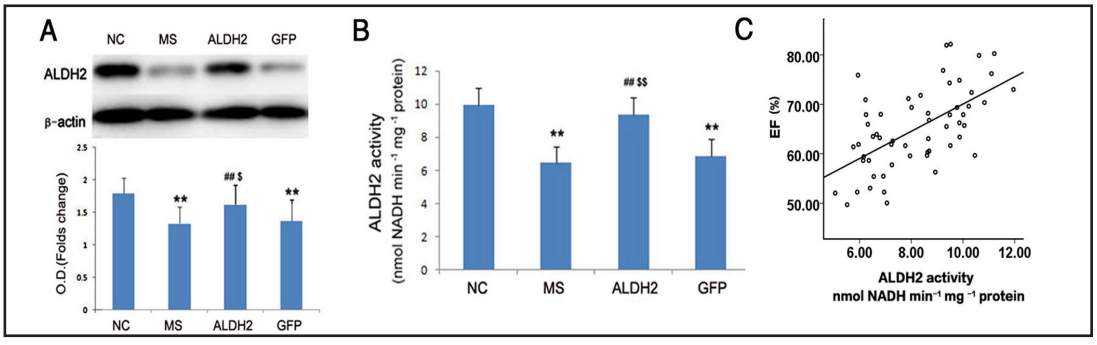

Fig. 1. Expression and activation of ALDH2 after injection of the lentiviral vector (A,B); correlation between ALDH2 activity and EF (C). Data are shown as the mean ± SEM. **P<0.01 vs. NC group; $^{\#\#}$P<0.01 vs. MS group; $^{\$}$ P<0.05 and $^{\$\$}$ P<0.01 vs. GFP group. NC group (n = 15); MS group (n = 14); ALDH2 group (n = 14); GFP group (n = 14).

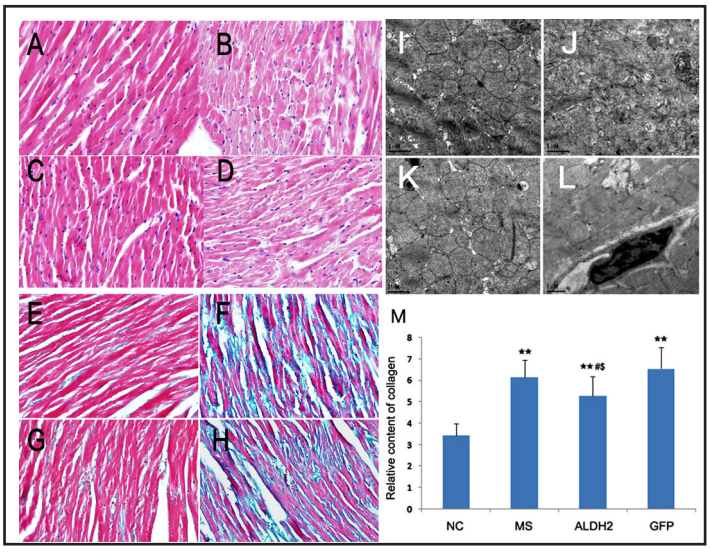

Fig. 2. Effect of ALDH2 on MS-induced changes in cardiac morphology. A, E, and I: NC group (n = 15); B, F, and J: MS group (n = 14); C, G, and K: ALDH2 group (n = 14); D, H, and L: GFP group (n = 14). HE staining indicated myocardial disorder in the MS group, with its alleviation in the ALDH2 group (×400) (A–D). Masson's trichrome staining of the sections revealed increased interstitial collagen deposition in the MS group, which was effectively prevented in the ALDH2 group (×400) (E–H). Transmission electron microscopy analysis showed swollen mitochondria in the cardiomyocytes of MS mice compared with NC mice; the ultrastructural changes in cardiomyocytes were ameliorated in the ALDH2 group (I–L). M: Comparison of the relative collagen content of the four groups of mice. Data are shown as the mean ± SEM. **P<0.01 vs. NC group; $^{\#}$P<0.01 vs. MS group; $^{\$}$ P<0.05 vs. GFP group.

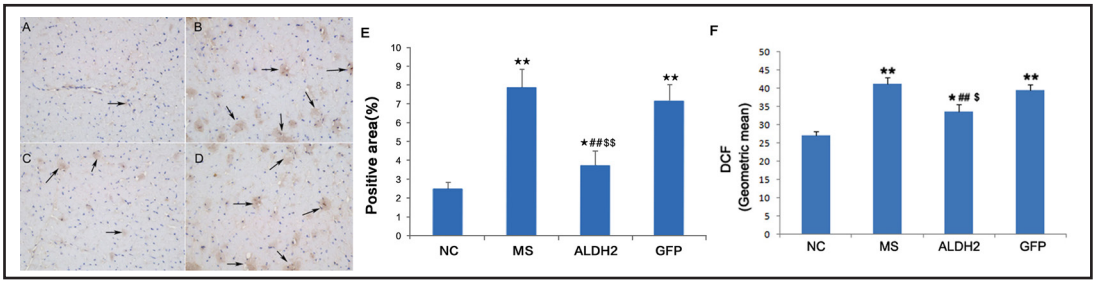

Fig. 3. A–D: Immunohistochemistry staining of 4-HNE in ventricular cross-sections. A: NC group (n = 10); B: MS group (n = 10); C: ALDH2 group (n = 14); D: GFP group (n = 14). The arrows indicate positive 4-HNE staining (×400). E: Quantitative analysis of the 4-HNE-positive area in the four groups. Data are shown as the mean ± SEM. *P<0.05 and **P<0.01 vs. NC group; $^{\#\#}$P<0.01 vs. MS group; $^{\$\$}$P<0.05 vs. GFP group. F: Quantitative analysis of ROS production detected with DCFH-DA in the four groups. Data are shown as the mean ± SEM. *P<0.05 and **P<0.01 vs. NC group.

ALDH2 attenuates MS-induced myocardial tissue damage

To assess the effects of ALDH2 overexpression on myocardial damage after chronic exposure to a HF diet, we examined heart morphology, collagen deposition, and cardiac ultrastructural changes. We observed a myocardial disorder in the MS mice, as evidenced by HE staining; this was attenuated in the ALDH2-overexpression group (Fig. 2A-D). Staining of cardiac sections with Masson's trichrome revealed increased interstitial collagen deposition after the induction of MS; however, interstitial collagen deposition was effectively prevented by ALDH2 overexpression (Fig. 2E–H, M). Transmission electron microscopy ultrastructural analysis revealed swollen mitochondria in the cardiomyocytes from the MS mice compared to cardiomyocytes from the NC mice; these ultrastructural changes were effectively improved by ALDH2 overexpression (Fig. 2I-L).

ALDH2 reduces MS-induced myocardial oxidative stress

To understand how ALDH2 overexpression attenuated myocardial damage, we examined myocardial oxidative stress. Myocardial ROS content and 4-HNE expression were significantly higher in the MS group than in the NC group (Fig. 3). After lentiviral vector-mediated ALDH2

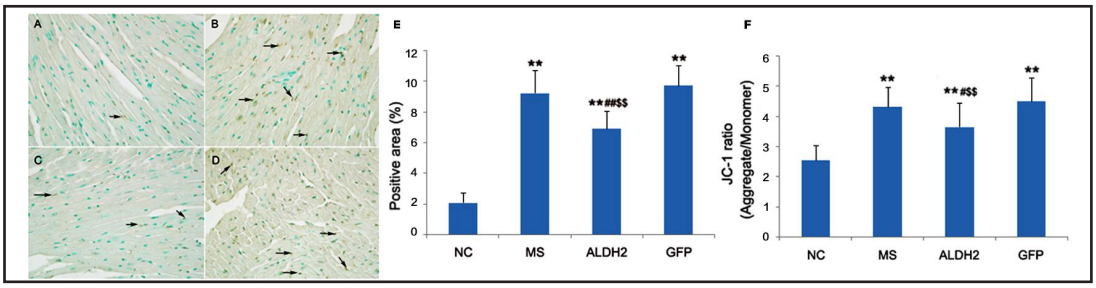

Fig. 4. A–D: TUNEL staining demonstrates apoptosis in cardiomyocytes. A: NC group (n = 10); B: MS group (n = 10); C: ALDH2 group (n = 14); D: GFP group (n = 14). The arrows indicate apoptotic cells (×400) E: Quantitative analysis of apoptotic cells. Data are shown as the mean ± SEM. *P<0.05 and **P<0.01 vs. NC group; ##P<0.01 vs. MS group; $$P<0.05 vs. GFP group. F: Quantitative analysis of the ΔΨm in the four groups. Data are shown as the mean ± SEM. *P<0.05 and **P<0.01 vs. NC group.

overexpression, 4-HNE expression decreased significantly (Fig. 3A–E), and ROS content was reduced, though not to statistical significance (Fig. 3F).

ALDH2 ameliorates MS-induced mitochondrial damage and apoptosis

Cardiomyocytes from mice in each group were examined for mitochondrial integrity and apoptosis. Abundant TUNEL-positive cells were observed in MS mice, but were significantly less frequent in the ALDH2-overexpression group (Fig. 4A–D). In addition, we observed significant loss of mitochondrial membrane potential in cardiomyocytes from the MS mice; the loss of mitochondrial membrane potential was attenuated in cardiomyocytes from mice in the ALDH2-overexpression group (Fig. 4F).

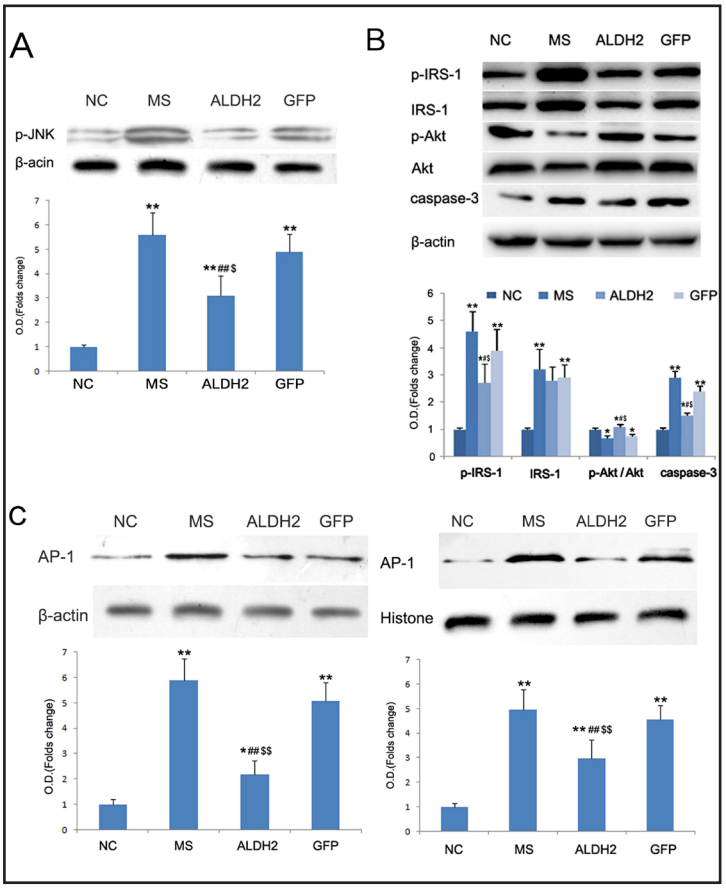

Fig. 5. Western blot analysis of JNK, AP-1, IRS-1, Akt, and caspase 3 in cardiac tissue. A: JNK phosphorylation. The upper panels show representative blots; the bottom bar graphs show relative protein levels.B: Expression levels of p-IRS-1, p-Akt, total IRS-1, total Akt, and caspase 3. The upper panels show representative blots; the bottom bar graphs show relative protein levels. C: Levels of total and nuclear AP-1. The upper panels show representative blots; the bottom bar graphs show relative protein levels. Each bar represents the mean ± SEM. *P<0.05 and **P<0.01 vs. NC group; #P<0.05 and ##P<0.01 vs. MS group; $P<0.05 and $$P<0.01 vs. GFP group. NC group (n= 15); MS group (n = 14); ALDH2 group (n = 14); GFP group (n = 14).

ALDH2 regulates the expression of JNK, AP-1, IRS-1, Akt and caspase 3 in cardiac tissue

To explore the possible mechanisms by which ALDH2 overexpression is protective against MS- induced myocardial damage, we evaluated the expression and phosphorylation of JNK, AP-1, IRS-1, Akt and the Akt downstream signaling molecule caspase 3. We found increased protein expression of JNK, AP-1, IRS-1, and caspase 3 and reduced Akt phosphorylation in cardiac tissues from the MS mice; these effects were mitigated in cardiac tissues from mice in the ALDH2-overexpression group (Fig. 5).

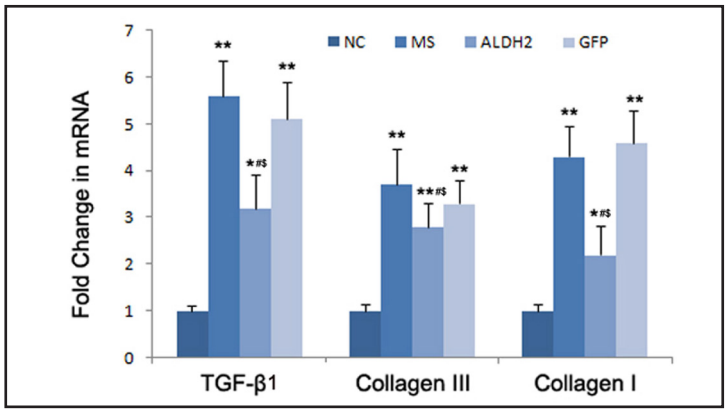

Fig. 6. PCR analysis of the mRNA expression of TGF-β1, collagen I and collagen III in cardiac tissue. Each bar represents the mean ± SEM. *P<0.05 and **P<0.01 vs. NC group; #P<0.05 vs. MS group; $P<0.05 vs. GFP group. NC group (n = 15); MS group (n = 14); ALDH2 group (n = 14); GFP group (n = 14).

ALDH2 regulates the expression of TGF-β1, collagen I and collagen III in cardiac tissue

To explore the possible mechanisms by which ALDH2 ameliorates MS-induced myocardial fibrosis, we examined the expression of TGF-β1 and collagen I and III in cardiac tissues. MS significantly upregulated the expression of collagen I and III and TGF-β1 in cardiac tissues; however, the downregulated expression of collagen I and III and TGF-β1 was observed in cardiac tissue from mice in the ALDH2-overexpression group (Fig. 6).

Discussion

In this study, we produced obesity and metabolic disturbances in mice fed a HF diet, which mimic human MS. Using this model, we demonstrated that MS caused significant myocardial lesions, increased myocardial apoptosis, and induced myocardial fibrosis. In addition, we revealed a cardioprotective role for ALDH2 against myocardial remodeling induced by a HF diet.

Our results demonstrated that lentiviral vector-mediated ALDH2 overexpression ameliorated myocardial damage induced by a HF diet, possibly by reducing oxidative stress and improving insulin resistance. Additionally, our study indicated crosstalk between JNK and AP-1 signaling pathways, converging on p-IRS-1 and leading to the inhibition of Akt phosphorylation and cell apoptosis. Another convergence point of the JNK and AP-1 pathways was TGF-β1 pathway, which promotes myocardial fibrosis in MS mice induced by a HF diet.

The hallmarks of lipotoxic cardiomyopathy include reduced contractility and deposition of lipid droplets in cardiomyocytes [21, 22]. We observed reduced EF and FS, enlarged LVEDD and LVESD, elevated IVSd and LVPWd, and excessive apoptosis, deposition of lipid droplets, and collagen fibers in cardiomyocytes of MS mice. Several mechanisms may be responsible for these MS-related abnormalities, including impaired insulin resistance and increased oxidative stress [23, 24]. In this study, impaired insulin resistance may underscore the accelerated apoptosis and myocardial fibrosis in cardiac tissue of MS mice induced by a HF diet. ALDH2 overexpression ameliorated HF diet-induced myocardial damage, consistent with previous findings that mitochondrial protection is beneficial against myocardial dysfunction induced by a HF diet [25, 26]. We observed increased apoptosis and loss of

mitochondrial membrane potential, along with upregulation of 4-HNE, in the hearts of mice with HF diet-induced MS, indicating a corroborative role of oxidative stress, apoptosis and mitochondrial dysfunction in lipotoxic cardiomyopathy [27].

Although ALDH2 overexpression alleviated aortic plaque development in apoE-/- mice [28], the effect of ALDH2 on lipotoxicity in the hearts of animals with MS is poorly understood. In this study we found that ALDH2 overexpression ameliorated HF diet-induced cardiac remodeling and contractile dysfunction, accompanied by improved mitochondrial integrity and myocyte survival. We suggest that the protective effect of ALDH2 is due to inhibition of JNK/AP-1 pathway. In the heart, both JNK and AP-1 are key regulators of myocardial remodeling [11, 29]. In addition, hypertension-induced cardiac dysfunction is associated with increased AP-1 activity [5]. In this study, we found that enhanced JNK phosphorylation and decreased Akt phosphorylation were associated with impaired cardiac function in response to the chronic consumption of a HF diet. JNK and Akt are essential for energy metabolism, cardiac survival, and contractile function [30, 31]. Our observation that ALDH2 inhibits JNK phosphorylation and compensates for the loss of Akt activation in response to a HF diet represents a possible connection between these pathways. The activation of AP-1 and JNK increases TGF-β1 expression and promotes myocardial fibrosis [32]. Therefore, JNK and AP-1 signaling may elicit apoptosis by reducing Akt phosphorylation, and may sensitize myocardial fibroblasts to pathophysiological changes.

In addition, the alteration of AP-1, which inhibits the transcription of α1 procollagen, is associated with increased collagen production [33]. Caspase 3 is a regulator of cell apoptosis and is involved in Akt-mediated anti-apoptotic mechanisms [34]. Our data demonstrate enhanced caspase 3 activity, mitochondrial damage, and myocardial fibrosis in MS mice but not in MS mice with ALDH2 overexpression. These data reveal a possible role for JNK and AP-1 in HF diet-induced mitochondrial dysfunction and cell apoptosis, and support a beneficial role for ALDH2. However, our data suggest an associative relationship between these signaling pathways, rather than a causal relationship; further study is needed to elucidate the functional role of AP-1, JNK, and Akt in mediating the cardioprotection provided by ALDH2.

In conclusion, this study reveals a crucial protective role for ALDH2 in the protection against HF diet-induced cardiac lipotoxicity. ALDH2 attenuates the cardiac dysfunction, apoptosis, oxidative stress and mitochondrial damage induced by a HF diet, possibly by inhibiting the activation of AP-1 and JNK and enhancing the phosphorylation of Akt. We conclude that ALDH2 is a potential therapeutic target that could be used in the management of MS.

Acknowledgements

This work was supported by the National Natural Science Foundation of China (No. 81400282 and 81570401), the Taishan Scholar Program of Shandong Province (No. 20130911 and 20161065), the Fund from Department of Science and Technology of Shandong Province (No. 2014GGH218004), the China Postdoctoral Science Foundation (No. 2017M612293), and the Shandong Province Postdoctoral Special Fund (No. 201402033). We thank Nathan Qi and Kavaljit Chhabra at University of Michigan for their language assistance.

Disclosure Statement

The authors confirm that they have no conflict of interests.

References

1 Yen HW, Lin HL, Hao CL, Chen FC, Chen CY, Chen JH, Shen KP: Effects of pre-germinated brown rice treatment high-fat diet-induced metabolic syndrome in C57BL/6J mice. Biosci Biotechnol Biochem 2017;81:979-986.
2 Furukawa S, Fujita T, Shimabukuro M, Iwaki M, Yamada Y, Nakajima Y, Nakayama O, Makishima M, Matsuda M, Shimomura I: Increased oxidative stress in obesity and its impact on metabolic syndrome. J Clin Invest 2004;114:1752-1761.
3 Diop SB, Bisharat-Kernizan J, Birse RT, Oldham S, Ocorr K, Bodmer R: PGC-1/Spargel Counteracts High-Fat-Diet-Induced Obesity and Cardiac Lipotoxicity Downstream of TOR and Brummer ATGL Lipase. Cell Rep 2015;10.1016/j.celrep.2015.02.022
4 Dirkx E, van Eys GJ, Schwenk RW, Steinbusch LK, Hoebers N, Coumans WA, Peters T, Janssen BJ, Brans B, Vogg AT, Neumann D, Glatz JF, Luiken JJ: Protein kinase-D1 overexpression prevents lipid-induced cardiac insulin resistance. J Mol Cell Cardiol 2014;76:208-217.
5 Li CB, Li XX, Chen YG, Zhang C, Zhang MX, Zhao XQ, Hao MX, Hou XY, Gong ML, Zhao YX, Bu PL, Zhang Y: Effects and mechanisms of PPARalpha activator fenofibrate on myocardial remodelling in hypertension. J Cell Mol Med 2009;13:4444-4452.
6 Zhang Y, Babcock SA, Hu N, Maris JR, Wang H, Ren J: Mitochondrial aldehyde dehydrogenase (ALDH2) protects against streptozotocin-induced diabetic cardiomyopathy: role of GSK3beta and mitochondrial function. BMC Med 2012;10:40.
7 Budas GR, Disatnik MH, Mochly-Rosen D: Aldehyde dehydrogenase 2 in cardiac protection: a new therapeutic target? Trends Cardiovasc Med 2009;19:158-164.
8 Doser TA, Turdi S, Thomas DP, Epstein PN, Li SY, Ren J: Transgenic overexpression of aldehyde dehydrogenase-2 rescues chronic alcohol intake-induced myocardial hypertrophy and contractile dysfunction. Circulation 2009;119:1941-1949.
9 Ebert AD, Kodo K, Liang P, Wu H, Huber BC, Riegler J, Churko J, Lee J, de Almeida P, Lan F, Diecke S, Burridge PW, Gold JD, Mochly-Rosen D, Wu JC: Characterization of the molecular mechanisms underlying increased ischemic damage in the aldehyde dehydrogenase 2 genetic polymorphism using a human induced pluripotent stem cell model system. Sci Transl Med 2014;6:255ra130.
10 Kim GJ, Song DH, Yoo HS, Chung KH, Lee KJ, An JH: Hederagenin Supplementation Alleviates the Pro-Inflammatory and Apoptotic Response to Alcohol in Rats. Nutrients 2017;9:
11 Szymanska E, Skowronek A, Miaczynska M: Impaired dynamin 2 function leads to increased AP-1 transcriptional activity through the JNK/c-Jun pathway. Cell Signal 2016;28:160-171.
12 Venkatesan B, Valente AJ, Prabhu SD, Shanmugam P, Delafontaine P, Chandrasekar B: EMMPRIN activates multiple transcription factors in cardiomyocytes, and induces interleukin-18 expression via Rac1-dependent PI3K/Akt/IKK/NF-kappaB andMKK7/JNK/AP-1 signaling. J Mol Cell Cardiol 2010;49:655-663.
13 Aminzadeh A: Protective effect of tropisetron on high glucose induced apoptosis and oxidative stress in PC12 cells: roles of JNK, P38 MAPKs, and mitochondria pathway. Metab Brain Dis 2017;32:819-826.
14 Bennett BL, Satoh Y, Lewis AJ: JNK: a new therapeutic target for diabetes. Curr Opin Pharmacol 2003;3:420-425.
15 Yariswamy M, Yoshida T, Valente AJ, Kandikattu HK, Sakamuri SS, Siddesha JM, Sukhanov S, Saifudeen Z, Ma L, Siebenlist U, Gardner JD, Chandrasekar B: Cardiac-restricted Overexpression of TRAF3 Interacting Protein 2 (TRAF3IP2) Results in Spontaneous Development of Myocardial Hypertrophy, Fibrosis, and Dysfunction. J Biol Chem 2016;291:19425-19436.
16 Li CB, Li XX, Chen YG, Gao HQ, Bao CM, Liu XQ, Bu PL, Zhang J, Zhang Y, Ji XP: Myocardial remodeling in rats with metabolic syndrome: role of Rho-kinase mediated insulin resistance. Acta Biochim Pol 2012;59:249-254.
17 Turdi S, Ge W, Hu N, Bradley KM, Wang X, Ren J: Interaction between maternal and postnatal high fat diet leads to a greater risk of myocardial dysfunction in offspring via enhanced lipotoxicity, IRS-1 serine phosphorylation and mitochondrial defects. J Mol Cell Cardiol 2013;55:117-129.
18 Wang S, Wang C, Turdi S, Richmond KL, Zhang Y, Ren J: ALDH2 protects against high fat diet-induced obesity cardiomyopathy and defective autophagy: role of CaM kinase II, histone H3K9 methyltransferase SUV39H, Sirt1, and PGC-1alpha deacetylation. Int J Obes (Lond) 2018;42:1073-1087.
19 Yamamoto W, Sakaguchi A, Origasa H, Yaginuma T, Kanazawa Y: [Relationship between insulin resistance and blood pressure]. Nihon Koshu Eisei Zasshi 1994;41:230-236.

20 Bellenger NG, Burgess MI, Ray SG, Lahiri A, Coats AJ, Cleland JG, Pennell DJ: Comparison of left ventricular ejection fraction and volumes in heart failure by echocardiography, radionuclide ventriculography and cardiovascular magnetic resonance; are they interchangeable? Eur Heart J 2000;21:1387-1396.
21 Chiu HC, Kovacs A, Blanton RM, Han X, Courtois M, Weinheimer CJ, Yamada KA, Brunet S, Xu H, Nerbonne JM, Welch MJ, Fettig NM, Sharp TL, Sambandam N, Olson KM, Ory DS, Schaffer JE: Transgenic expression of fatty acid transport protein 1 in the heart causes lipotoxic cardiomyopathy. Circ Res 2005;96:225-233.
22 Park TS, Goldberg IJ: Sphingolipids, lipotoxic cardiomyopathy, and cardiac failure. Heart Fail Clin 2012;8:633-641.
23 Mollica MP, Mattace Raso G, Cavaliere G, Trinchese G, De Filippo C, Aceto S, Prisco M, Pirozzi C, Di Guida F, Lama A, Crispino M, Tronino D, Di Vaio P, Berni Canani R, Calignano A, Meli R: Butyrate Regulates Liver Mitochondrial Function, Efficiency, and Dynamics in Insulin-Resistant Obese Mice. Diabetes 2017;66:1405-1418.
24 Pakdeechote P, Bunbupha S, Kukongviriyapan U, Prachaney P, Khrisanapant W, Kukongviriyapan V: Asiatic acid alleviates hemodynamic and metabolic alterations via restoring eNOS/iNOS expression, oxidative stress, and inflammation in diet-induced metabolic syndrome rats. Nutrients 2014;6:355-370.
25 Manrique C, DeMarco VG, Aroor AR, Mugerfeld I, Garro M, Habibi J, Hayden MR, Sowers JR: Obesity and insulin resistance induce early development of diastolic dysfunction in young female mice fed a Western diet. Endocrinology 2013;154:3632-3642.
26 Littlejohns B, Pasdois P, Duggan S, Bond AR, Heesom K, Jackson CL, Angelini GD, Halestrap AP, Suleiman MS: Hearts from mice fed a non-obesogenic high-fat diet exhibit changes in their oxidative state, calcium and mitochondria in parallel with increased susceptibility to reperfusion injury. PLoS One 2014;9:e100579.
27 Yokoyama M, Yagyu H, Hu Y, Seo T, Hirata K, Homma S, Goldberg IJ: Apolipoprotein B production reduces lipotoxic cardiomyopathy: studies in heart-specific lipoprotein lipase transgenic mouse. J Biol Chem 2004;279:4204-4211.
28 Pan C, Xing JH, Zhang C, Zhang YM, Zhang LT, Wei SJ, Zhang MX, Wang XP, Yuan QH, Xue L, Wang JL, Cui ZQ, Zhang Y, Xu F, Chen YG: Aldehyde dehydrogenase 2 inhibits inflammatory response and regulates atherosclerotic plaque. Oncotarget 2016;7:35562-35576.
29 Erikson JM, Valente AJ, Mummidi S, Kandikattu HK, DeMarco VG, Bender SB, Fay WP, Siebenlist U, Chandrasekar B: Targeting TRAF3IP2 by Genetic and Interventional Approaches Inhibits Ischemia/Reperfusion-induced Myocardial Injury and Adverse Remodeling. J Biol Chem 2017;292:2345-2358.
30 Khairallah M, Khairallah R, Young ME, Dyck JR, Petrof BJ, Des Rosiers C: Metabolic and signaling alterations in dystrophin-deficient hearts precede overt cardiomyopathy. J Mol Cell Cardiol 2007;43:119-129.
31 Musi N, Goodyear LJ: Insulin resistance and improvements in signal transduction. Endocrine 2006;29:73-80.
32 Shyu KG, Wang BW, Chen WJ, Kuan P, Hung CR: Mechanism of the inhibitory effect of atorvastatin on endoglin expression induced by transforming growth factor-beta1 in cultured cardiac fibroblasts. Eur J Heart Fail 2010;12:219-226.
33 Jacques E, Semlali A, Boulet LP, Chakir J: AP-1 overexpression impairs corticosteroid inhibition of collagen production by fibroblasts isolated from asthmatic subjects. Am J Physiol Lung Cell Mol Physiol 2010;299:L281-287.
34 Moon DO, Park SY, Choi YH, Kim ND, Lee C, Kim GY: Melittin induces Bcl-2 and caspase-3-dependent apoptosis through downregulation of Akt phosphorylation in human leukemic U937 cells. Toxicon 2008;51:112-120.